

Dislocation Nucleation in Shocked fcc Solids: Effects of Temperature and Preexisting Voids

Takahiro Hatano

Institute for Materials Research, Tohoku University, Sendai, 980-8577 Japan

(Received 14 January 2004; published 19 August 2004)

Quantitative behaviors of shock-induced dislocation nucleation are investigated by means of molecular dynamics simulations on fcc Lennard-Jones solids: a model argon. In perfect crystals, it is found that the Hugoniot elastic limit (HEL) is a linearly decreasing function of temperature: from near-zero to melting temperatures. In a defective crystal with a void, dislocations are found to nucleate on the void surface. Also, HEL drastically decreases to 15% of the perfect crystal when the void radius is 3.4 nanometers. The decrease of HEL becomes larger as the void radius increases, but HEL becomes insensitive to temperature.

DOI: 10.1103/PhysRevLett.93.085501

PACS numbers: 62.20.Fe, 62.50.+p

Mechanical properties of shock-loaded solids are important to materials science since they can reveal reliability of materials under extreme conditions. Shocks in solids generate high pressure almost instantaneously, and create extremely high deformation (strain) rates. Yielding phenomena realized at high strain rates are usually quite different from those of quasistatic ones. Notably, Rohde has found that the HEL (Hugoniot elastic limit) is almost independent of temperature [1]; Kanel and his coworkers have found that the HELs of Al and Cu single crystals are increasing functions of temperature [2]. These experiments are in apparent contrast with quasistatic deformations, where yield strength considerably decreases with increasing temperature. However, contrary to Rohde and Kanel, stainless steel shows that the HEL is a decreasing function of temperature [3]. These puzzling results provide us with intriguing problems. The microscopic foundations of plastic deformation are dominated by the dynamics of dislocations. Unfortunately, the nature of dislocation dynamics is very complicated and yet to be fully understood from a theoretical point of view. Therefore, it is reasonable to decompose the problem into three essential ingredients of dislocation dynamics: nucleation, mobility, and multiplication. As the first stage of this line of thought, the properties of dislocation nucleation are investigated in this Letter.

In a perfect crystal, dislocations nucleate with the help of thermal fluctuations. Holian and Lomdahl have studied the emergence of stacking faults initiated by partial dislocation emission in a shocked perfect crystal [4]. Recently, Tanguy *et al.* [5] have performed extensive simulations to confirm that there exists a critical size of dislocation loop below which nucleated loops are energetically unstable and eventually annihilate; this is reminiscent of droplet nucleation in a metastable gas or liquid. Although these two studies are enlightening, the role of temperature, which is known to be important to dislocation nucleation, has not been considered. In some studies, temperature plays no role in activating dislocation nucleation [6]. However, dislocation nucleation seems to be

anyhow a fluctuation-assisted process in the sense that no nucleation is observed in a molecular dynamics simulation of a perfect crystal at zero temperature [4]. It is important to understand temperature effects on dislocation nucleation to clarify the controversial experimental results [1–3].

This Letter discusses temperature effects on dislocation nucleation through molecular dynamics simulations. It turns out that the HEL is a linearly decreasing function of temperature from zero to melting temperatures. Then a defect is introduced into the system as a preexisting void, at which dislocation nucleation is found to be enhanced.

The present simulations use a simple Lennard-Jones (LJ) potential $U(r) = 4\epsilon[(\sigma/r)^{12} - (\sigma/r)^6]$ with a cutoff length of 4.0σ . To avoid a discontinuity at the cutoff, the potential is suitably shifted. Note that simulations with shorter cutoffs such as 2.6σ resulted in a visible decrease of HEL, as much as 90%. Hereafter, we let $\sigma = 3.41 \text{ \AA}$ and $\epsilon = 1.65 \times 10^{21} \text{ J}$ in order to make a quantitative comparison with experiments on solid argon. The Lennard-Jones potential has been well tested in terms of mechanical and thermal properties of argon such as the elastic constants and the melting temperature. Hence it is reasonable to adopt the LJ potential as the first computational attempt to understand the anomalous HEL behavior of fcc metals [2].

In our system, the axes of x , y , and z are taken to coincide with $\langle 100 \rangle$, $\langle 010 \rangle$, and $\langle 001 \rangle$ directions, respectively. Shocks propagate along the $[001]$ direction. As usual, periodic boundary conditions are applied to x and y directions. The whole system consists of $100 \times 100 \times 200$ unit cells. Shock waves in the present simulations are generated by pushing a piston of infinite mass into the still target. The velocity of the piston is denoted by u_p . We call the piston velocity u_p throughout this Letter.

In this Letter, the HEL is defined as the longitudinal stress (σ_{zz}) above which dislocation nucleation is observed. Note that this definition of HEL differs from the

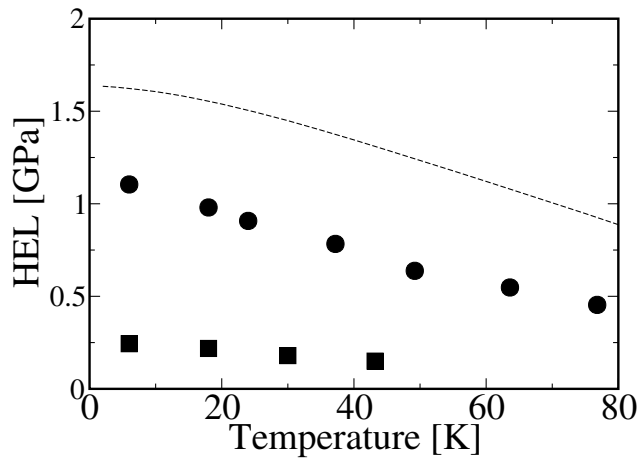


FIG. 1. Temperature dependence of Hugoniot elastic limits of a perfect crystal (circles) and of a defective crystal containing a void of 1.71 nm radius (squares). The dashed line represents experimental data for the shear modulus [8]. The melting temperature is approximately 83 K.

one that is based entirely on shock wave behavior: the shock front decomposes into an elastic precursor and a plastic wave. However, these two definitions are identical because the decomposition is also observed in molecular dynamics simulations once dislocations are emitted in shocked solids. Longitudinal stress is calculated from the Hugoniot relation; $\sigma_{zz} = \rho_0 u_s u_p$, where ρ_0 and u_s denote initial density and shock velocity, respectively. Note that the initial pressure is zero. The longitudinal stress σ_{zz} is approximately proportional to the shear stress [4] which is directly responsible for dislocation emission.

Figure 1 shows the nearly linear dependence of HEL on temperature. The HEL at 77 K, close to the melting temperature (83 K) [7], is approximately half that at 6 K. This is clear evidence that dislocation nucleation is a thermally assisted phenomenon. Also, this temperature dependence is reminiscent of elastic constants. The dashed line in Fig. 1 represents the shear modulus of solid argon [8]. We can see that the temperature dependences of the HEL and of the shear modulus are qualitatively the same for perfect crystals. That is, HEL is approximately half the shear modulus regardless of temperature. (Indeed, the ratio of HEL to shear modulus is slightly greater than 0.5 for $T \leq 24$ K.) The critical strain also decreases linearly from 0.138 (at 6 K) down to 0.118 (at 77 K) as the temperature increases. Numerical data are shown in Table I. Note that the temperature dependence of the shear modulus of argon has been calculated by molecular dynamics simulation using LJ potential [9].

The temperature dependence of HEL obtained by the present simulation is opposite to the experiment on fcc metals [2]. But this is not a contradiction, for the experiment involves real crystals where various defects and impurities preexist. Plastic deformations of real materials

TABLE I. Critical piston velocity, Hugoniot elastic limit, and critical strain for the perfect crystal as functions of initial temperature.

Initial Temperature K	Critical Piston Velocity m/sec	HEL GPa	Critical Strain %
6	291	1.08	13.8
18	275	0.957	13.7
24	261	0.886	13.1
37	243	0.765	13.0
49	216	0.623	12.3
64	202	0.535	12.2
77	186	0.443	11.8

are mainly governed by the motion of preexisting dislocations, while in a perfect crystal, only the dislocation nucleation is considered here. Hence, the mobility of preexisting dislocations must be analyzed for further understanding of temperature dependence of shock-induced plasticity. This subject will be discussed elsewhere.

Strikingly different results are found when we turn to defective crystals, concentrating on the effects of a void. A void is introduced in a model crystal as a blanked spherical region. The radius is varied from 0.34 nm to 3.41 nm. With a void, dislocations nucleate exclusively on the void surface as shown in Figs. 2–4.

The Hugoniot elastic limit decreases drastically in the presence of a void. Square symbols in Fig. 1 represent the HEL for a defective crystal with a void of 1.71 nm radius. With this size of void, the HEL is approximately 20% of the perfect crystals. Note that the HEL of a defective

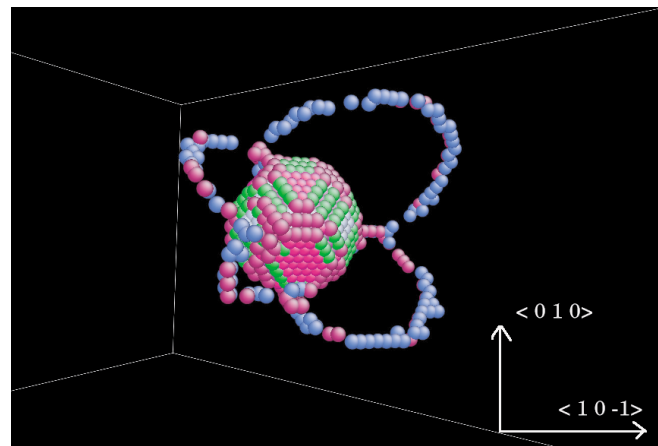


FIG. 2 (color online). Four partial dislocation loops nucleate on the void surface. Void radius is 2.4 nm and piston velocity is 70 m/s. Atoms of 12 nearest neighbors are not presented in order to see exclusively dislocations and void surface. Green, red, and blue atoms have 10, 11, and 13 nearest neighbors, respectively [15].

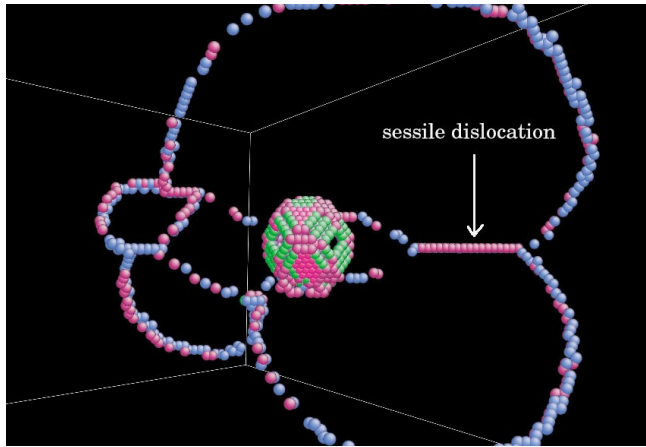


FIG. 3 (color online). Thirteen picoseconds after Fig. 2. Partial dislocation loops are extended and Lomer-Cottrell sessile dislocation is formed.

crystal also linearly decreases with increasing temperature up to 42 K.

When $T > 42$ K, approximately half the melting temperature, no dislocation is nucleated and a void collapses after the passage of shock front. Although this phenomenon is similar to “hot spot” formation [10], this is not the case since the piston velocity used here is not strong enough to cause a jet which is essential to hot spot. The collapse of the void observed in the present situation rather postulates that voids are unstable to perturbations above half the melting temperature [11].

Below 42 K, the HEL and the critical piston velocity for the defective crystal with a void become insensitive to temperature. For the case of $r = 1.02$ nm, the critical piston velocity is 103 ± 5 m/s at 6 K, dropping only to 95 ± 5 m/s at 42 K, while for the perfect crystal, the corresponding values are 289 ± 1.6 m/s and 213 ± 1.6 m/s, respectively. The absolute decreases are 8 m/s

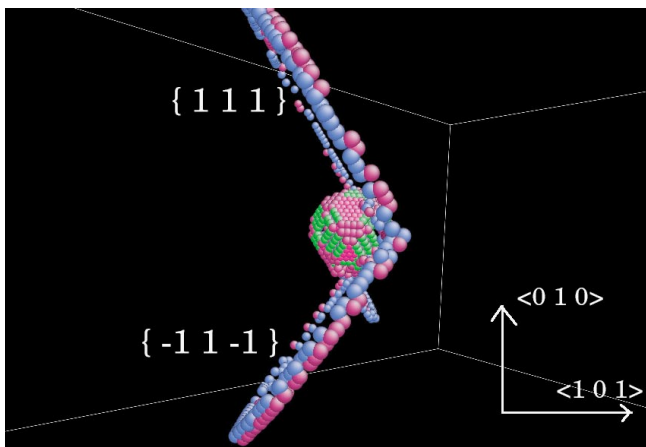


FIG. 4 (color online). Side view of Fig. 3. Two slip planes on the void surface are activated.

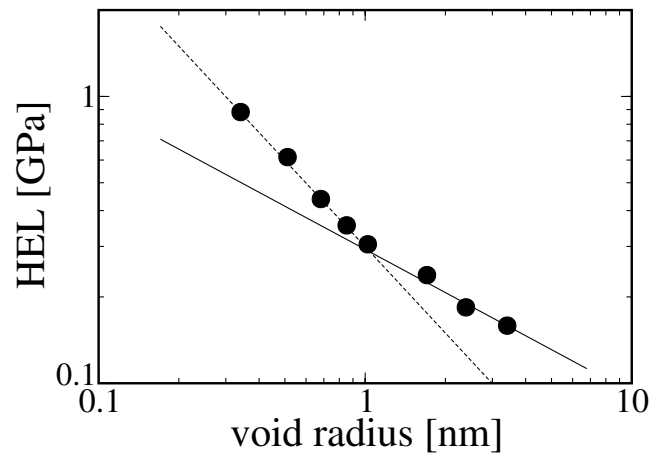


FIG. 5. Log-log plot of HEL as a function of void radius. Solid and dashed lines are proportional to $r^{-0.5}$ and r^{-1} , respectively. Initial temperature is 6 K.

for the defective crystal and 76 m/s for the perfect crystal. Then the relative changes are $8/103 \approx 0.08$ and $76/284 \approx 0.26$, respectively. The difference between the perfect and the defective crystals is remarkable in terms of both absolute and relative decreases. Thus, defects dominate thermal fluctuations in the enhancement of dislocation nucleations. In experiment, the microstructure of the specimen is important.

The void-size dependence of HEL is shown in Fig. 5. At small r , the HEL decreases as r^{-1} followed by a crossover to $r^{-0.5}$ at $r_c = 1.3 \pm 0.3$ nm. Note that the transition radius r_c is approximately the width of a double kink and is also very close to the critical loop radius 1.5 nm above which nucleated dislocation loops grow stably [5]. The quantitative explanation of this intriguing transition is not clear at this point.

To compare the present simulation with experiment, the Hugoniot values (u_p versus u_s) of argon for both this simulation and experiment [12] are presented in Table II. We see that the simulation values exceed the experimental

TABLE II. Comparison of simulation and experimental shock velocities as functions of piston velocity. (Simulation data involves a perfect crystal.) Initial temperature and density for the simulation are 64 K and 1.63 g/cc, respectively, while they are 75 K and 1.65 g/cc in the experiment.

Piston Velocity km/sec	Shock velocity	
	(Experiment) km/sec	(Simulation) km/sec
0.56	2.00	2.35
0.78	2.44	2.77
0.94	2.68	3.01
1.29	3.53	3.82
1.78	4.17	4.82

ones by approximately 15%. This overestimation is comparable to that of Belonoshko's simulations using a Buckingham potential [13]. His deviation from the experimental value exceeds 10%, especially for small piston velocities up to 1.2 km/sec. Dubrovinsky has attributed this overestimation to the polycrystalline nature of the experimental specimen [14]. Since both Belonoshko's and the present simulations deal only with crystals of $\langle 100 \rangle$ orientation, the deviation from the experimental result is not unreasonable.

Finally, two quantitative uncertainties in the present simulation are remarked. One is the underestimation of stacking fault energy by the use of LJ potential. It is known that stacking fault energy vanishes when one adopts short-range, two-body intermolecular potentials [14]. In this regard, it is possible that the numerical values of the HEL obtained by the present simulations are underestimates. But at least qualitative results such as the temperature dependence or the void effect are not so influenced by the nature of two-body potentials. In addition, a large cutoff, 4.0σ , was used to reduce this effect.

The other uncertainty involves periodic boundary conditions. The system size ($57 \times 57 \times 114$ nm) is small enough that a dislocation loop may interact with itself through the periodic boundary conditions. It is impossible to remove this uncertainty from molecular dynamics simulations at this point. However, the strain around a nucleated dislocation loop propagates at the sound velocity (about 900 m/s for transverse mode), taking 45 picoseconds to cross the simulation cell. Therefore, this effect may not seriously influence the present results, which involve exclusively nucleation processes that occur within ten picoseconds.

To summarize, molecular dynamics simulations on both perfect and defective fcc crystals are performed from near-zero to melting temperatures. It is found that the Hugoniot elastic limit is about half the shear modulus and decreases linearly with increasing temperature. The critical piston velocity and critical strain also decrease in the same manner. When a void is introduced in the crystal, dislocations are found to nucleate on the void surface. The critical piston velocity decreases drastically as the void radius r increases. The decrease is nonlinear and shows a crossover from r^{-1} to $r^{-0.5}$ around $r \approx 1.3$ nm,

which is approximately the width of a double kink. The Hugoniot elastic limit becomes insensitive to temperature in the presence of a void. That is, the effect of nucleation at a void dominates that of thermal fluctuations in shock-induced dislocation nucleation.

The author gratefully acknowledges helpful discussions with H. Kaburaki, F. Shimizu, Y. Satoh, N. Nita, and H. Matsui.

-
- [1] R.W. Rohde, *Acta Metall.* **17**, 353 (1969).
 - [2] G. I. Kanel, S.V. Razorenov, K. Baumung, and J. Singer, *J. Appl. Phys.* **90**, 136 (2001); S.V. Razorenov, G. I. Kanel, K. Baumung, and H. J. Bluhm, in *Shock Compression of Condensed Matter—2001*, edited by M. D. Furnish, N. N. Thadani, and Y. Horie, AIP Conf. Proc. No. 620 (AIP, New York, 2002), p. 503.
 - [3] Z. Gu and X. Jin, in *Shock Compression of Condensed Matter—1997*, edited by S. C. Schmit *et al.*, AIP Conf. Proc. No. 429 (AIP, New York, 1998), p. 467.
 - [4] B. L. Holian and P. S. Lomdahl, *Science* **280**, 2085 (1998).
 - [5] D. Tanguy, M. Mareschal, P. S. Lomdahl, T. C. Germann, B. L. Holian, and R. Ravelo, *Phys. Rev. B* **68**, 144111 (2003).
 - [6] G. Xu and A. S. Argon, *Philos. Mag. Lett.* **80**, 605 (2000).
 - [7] R. Agrawal and D. A. Kofke, *Mol. Phys.* **85**, 43 (1995); M. A. van der Hoef, *J. Chem. Phys.* **113**, 8142 (2000).
 - [8] G. J. Keeler and D. N. Batchelder, *J. Phys. C* **3**, 510 (1970).
 - [9] F. Shimizu, H. Kimizuka, H. Kaburaki, J. Li, and S. Yip, *Proceedings of the Fourth International Conference on Supercomputing in Nuclear Applications, Tokyo, Japan, September 2000* (unpublished).
 - [10] T. Hatano, *Phys. Rev. Lett.* **92**, 015503 (2004) and references therein.
 - [11] Stability of a void at high temperatures is important in the context of irradiated materials. See, for example, J. Gittus, *Irradiation Effects in Crystalline Solids* (Applied Science Publishers Ltd., London, 1978).
 - [12] R. D. Dick, R. H. Warnes, and J. Skalyo, *J. Chem. Phys.* **53**, 1648 (1970).
 - [13] A. B. Belonoshko, *Science* **275**, 955 (1997).
 - [14] L. S. Dubrovinsky, *Science* **278**, 1474 (1997).
 - [15] Visualizations of atomistic configurations in this paper (Figs. 2–4) are produced by a free software ATOMEYE; J. Li, *Modell. Simul. Mater. Sci. Eng.* **11**, 173 (2003).